CORRELATING q_{net} TO E_{OED} OF PALEOGENE CLAYS OF VERY HIGH PLASTICITY

N. Okkels[1], L. Bødker[1], E. Skouboe[1] and T. Thorsen[1]

KEYWORDS

Clay, Oedometer modules, Cone resistance, Correlation, Lateral earth pressure

ABSTRACT

This paper provides practical formulations for correlating CPTu cone resistance q_c and net corrected cone resistance q_{net} to the oedometer reloading stiffness E_{OED} in highly overconsolidated, fissured, marine Paleogene clays of very high plasticity, from late Eocene and early Oligocene as observed in the Aarhus Denmark.

CPTu measurements provide detailed insights into both soil stratigraphy and geotechnical engineering properties. CPTu's carried out in these Paleogene clay types indicate very variable and fluctuating geotechnical properties spatially.

E_{OED} is determined from oedometer tests and is traditionally used for soil deformation analysis using a Mohr-Coulomb soil model. However, oedometer tests are time-consuming and expensive to perform. In practice, it is rarely possible to carry out a sufficient number of tests per site taking into account the variability and the financial framework. Therefore, it is essential to improve the statistical basis by including a priori knowledge of the stiffness parameters.

By correlation of E_{OED} from 73 oedometer tests with associated q_c- and q_{net}-values from CPTu's carried out near the boreholes from which the oedometer-samples are extracted linear correlations between these properties are found.

The correlations make it possible to derive E_{OED} directly from CPTu for use in the preliminary analysis of deformations. More importantly, the correlations support the final derivation of E_{OED} for 3D soil models once the results of all field and laboratory tests for the construction project are incorporated into the correlations.

[1] Geo, Aarhus, Denmark.

1. INTRODUCTION

Traditionally, odometer tests are used in commercial geotechnical surveys to determine the reload stiffness E_{OED} for use in a Mohr-Coulomb soil model. In recent years, the test is also used to support the derivation of the coefficient of lateral earth pressure K_0.

The reload stiffness E_{OED} should not be confused with the input parameter E_{oed} for a Plaxis model. E_{oed} in Plaxis' Hardening Soil model is a stiffness parameter dedicated to primary loading under oedometric conditions - i.e. the soil is in a normally consolidated state and lateral expansion is prevented during testing. Unfortunately, internationally the same nomenclature is used for the stiffness determined by the oedometer test - regardless of whether the soil is in a normal consolidated or overconsolidated state. Following the latter nomenclature, E_{OED} is defined in this paper as the stiffness of highly consolidated clays under reloading from the in situ stress level.

At the same time, CPTu has become the preferred investigation method because it is the most effective way to shed light on how stratigraphy, strength and stiffness vary spatially. To exploit this commercially, Geo has correlated q_c and q_{net} with the drained triaxial unloading and reloading stiffness E_{ur} [4] and the maximum small-strain shear modulus G_0 as well [5].

The CPTu's are performed in a single continuous stroke from the ground surface to target depth using Geo's enhanced CPT-system, which reduce the friction on the rod and make it possible to push the cone through more than 80 meters of very firm Paleogene clays.

Geo's CPT-crawler with a maximum push capacity of 15 ton is used together with a 10 or 15 cm^2 piezoelectric cone from the manufacturer A.P. van den Berg. The equipment and the execution agree with ISO 22476-1 with continuous measurement of tip resistance, sleeve friction, pore pressure (measured behind the tip of the probe) and inclination of the probe.

The CPTu's are supplemented with a few geotechnical boreholes for use in interpreting the CPTu's and for extracting soil samples for classification tests and advanced laboratory tests.

2. THE PALEOGENE STRATIFICATION

In costal parts of Aarhus, the Paleogene stratification is found near the surface only covered by fill and/or a thin series of glacial and or postglacial layers. The following Paleogene stratification is typically found, cf. figure 1:

Topmost 5-9 meter Viborg Clay, which is an Oligocene clay of very high plasticity with mica.

The Viborg clay is underlain by 0.5-2 m Kysing Marl, which is a highly glauconitous, highly calcareous, and high plasticity clay from the top of the

Eocene Søvind Marl formation. It is quite similar to the underlying Søvind Marl, but the geotechnical properties are typically better.

Below the Kysing Marl typically 9 to 13 meters of Moesgaard Clay - which is an Eocene clay of very high plasticity with mica - is found. This clay is somewhat reminiscent of the overlying Viborg Clay - both in terms of appearance and geotechnical properties. In some contexts, it is therefore not possible to distinguish these two clay types from each other by the eye. In such cases, the trivial name "Septarian Clay" is traditionally used for both clay types.

Søvind Marl underlies Moesgaard Clay. Søvind Marl is a clay of very high plasticity that makes up the majority of the Søvind Marl formation. It is predominantly very calcareous. However, calcareous-free or slightly calcareous zones frequently alternate with more calcareous ones.

All these clays are deposited in deep oceans and except for Kysing Marl, they are all fissured with slickensides. Due to the removal of younger layers by erosion and the weight of numerous glaciers during the Quaternary period, they are also highly overconsolidated with a geological preconsolidation stress greater than two MPa.

Large variations in plasticity and calcium carbonate content indicate that also strength and deformation properties vary a lot down through the formations. Variability in CPTu cone resistance confirms this, cf. figure 1. If cone resistance is decomposed into a trend component and a fluctuating component, the CPTu's shows that the fluctuating component is characterized by frequent and violent fluctuations around a trend line. Through the Septarian clays, the trend line is directly proportional to depth, but in the Søvind Marl it varies in large irregular cycles.

The oedometer modules of overconsolidated fine soils are traditionally described by a linear function of the minimum vertical effective stress that the clay has geologically experienced. Accordingly, E_{OED} increases linearly with depth. The corresponding function is derived based on oedometer tests performed with three unloading path to different minimum stresses. An oedometer stiffness is derived for each unloading for use in a mathematical overdetermination of the two coefficients of the function.

In accordance with the traditional model, the trend component in Figure 1 indicates that E_{OED} increases with depth in the Septarian Clays, while this does not seem to be the case for the Søvind Marl. Furthermore, the fluctuating component in Figure 1 indicates that also the stiffness of both clay types fluctuates violently over short distances, which the traditional model does not predict. The same is likely to apply the coefficients in the above-men-

tioned function of minimum vertical effective stress. The traditional approach therefore seems unsuitable for overconsolidated Paleogene clay types.

Seismic CPTu, where the maximum small-strain shear modulus G_0 is calculated from the measured shear wave velocity and compared directly with the cone resistance in the same position, documents that G_0 is proportional to the cone resistance [5]. It is reasonable to assume that this also applies to other stiffness modules including E_{OED}.

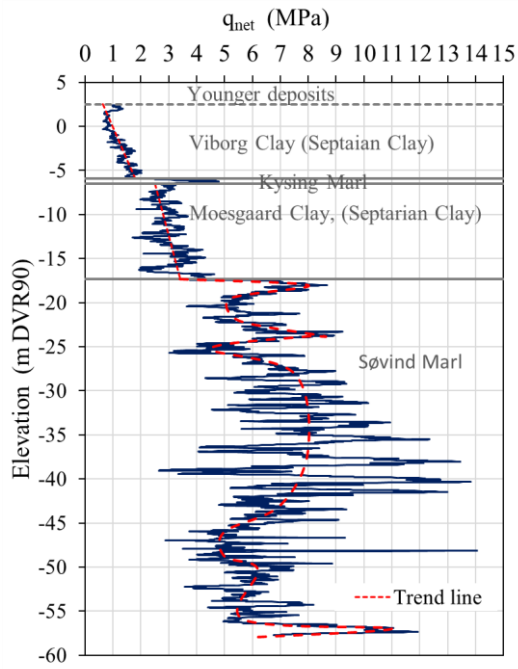

Figure 1. An example of a q_{net}-profile calculated from one of 36 CPTu's included in this study.

3. TEST PROCEDURES

The odometer tests are carried out following the guidelines specified in ISO 17892-5. All samples are extracted from Shelby-tube samples with an inner diameter of 70 mm.

Tests carried out with the very high plasticity Palaeogene clays usually begin with a measurement of the swell pressure, defined as the vertical pressure to be applied to the sample in the oedometer apparatus to prevent the sample from swelling when applied to water. The swell occurs because the in situ mean stress has not been restored in the oedometer apparatus.

After a sample is formed and installed in the oedometer apparatus, it is applied a vertical pressure slightly lower than the estimated effective vertical in

situ stress. When the sample is at rest at this load, water is added to the sample, and the swelling pressure is measured by recording the vertical pressure to be applied to the sample to prevent it from deforming (volume constancy) as shown in Figure 2. To prevent the tests from being significantly affected by osmosis forces [6], it is aimed to use apparatus water with the same salinity as the formation water.

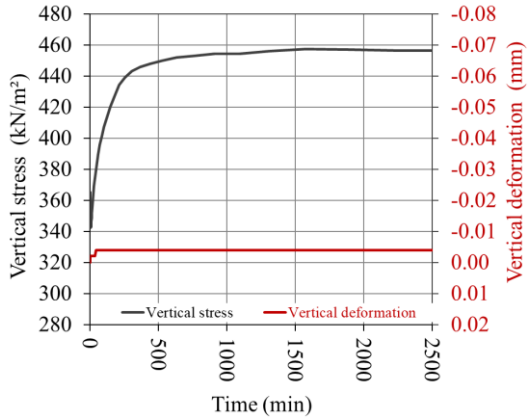

Figure 2. A swell pressure measurement in the oedometer apparatus.

During the preparation and installation of the sample, a negative pore pressure holds it together. Assuming volume constancy the coefficient of lateral earth pressure K_0 = 1.0 while water is added to the sample and the vertical swelling pressure is measured. Therefore, the measured swelling pressure approximately must represent the in situ mean stress σ'_{mean}. This means the in situ K_0 can be calculated from the definition of the mean stress: $\sigma'_{mean} = \sigma'_{v0}(1+2K_0)/3$, where σ'_{v0} is the estimated vertical effective in situ stress. However, this method is only applicable when in situ $K_0 > 1.0$.

Once the swelling pressure has been measured, the test is continued by loading the sample to a cautiously estimated geological preload stress determined as approximately 2.5 times the field vane strength measured by a fast field vane test (ISO 22476-9). This is done partly to minimize the effect of the inevitable test disturbance and partly to restore the in situ stress state. Next, the sample is unloaded to about the vertical effective in situ stress, after which it is reloaded to the previous maximum load. Finally, the sample is unloaded to the chosen minimum vertical effective stress. Figure 3 shows a typical stress-strain curve.

To facilitate a consistent derivation of the reloading stiffness, it is chosen to determine E_{OED} from the reloading curve by a polynomial fit to test data for an additional stress of 100 kPa to the minimum vertical effective unloading stress.

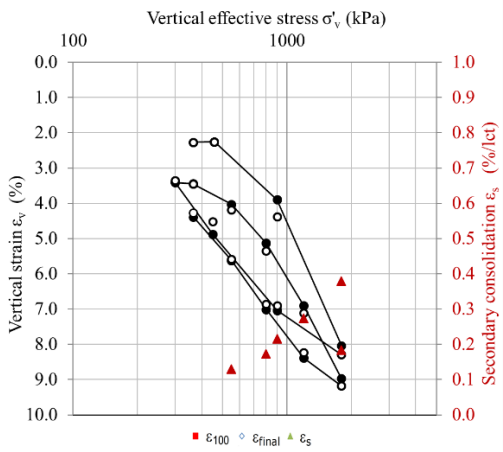

Figure 3. Example of an oedometer test.

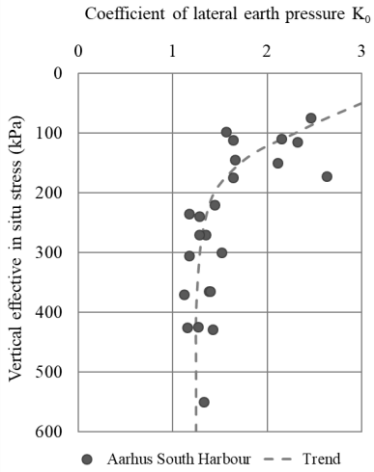

Figure 4. Example of K_0 calculated from swell pressure measurements.

As shown in Figure 5, the polynomial fit completely ignores the last point on the unloading curve. This is because this loading stage is strongly influenced by friction on the sides of the sample, which is working in the opposite direction to the friction during reloading. At the same time, the reloading is initiated before the creep at this stage has reversed direction.

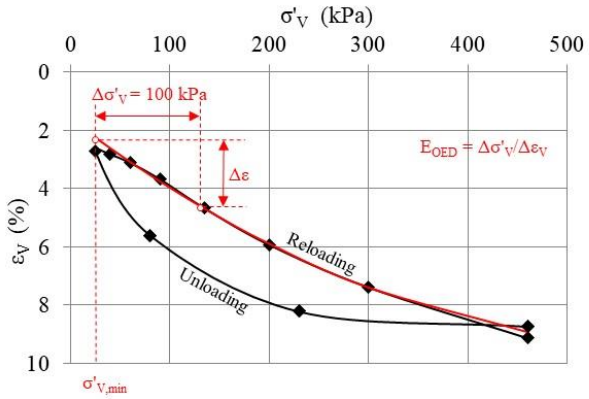

Figure 5. Principle of interpretation of the reloading stiffness E_{OED}.

The test samples are characterized by the soil index properties in Table 1.

The reload stiffness E_{OED} from the Septarian Clay tests is presented in Figure 6 and recorded in Figure 7 as a function of the minimum effective unloading stress $\sigma'_{v,min}$ during testing. The result show as expected a clear rectilinear trend:

$$E_{OED} \approx a \cdot \sigma'_{v,min} + b \quad (1)$$

where a and b are constants.

Geo ID	I_P	σ'_{v0}	σ'_{swell}	$\sigma'_{v,min}$	E_{OED}	a	E_{OED_insitu}	q_{net}	q_c
	%	kPa	kPa	kPa	MPa		MPa	MPa	MPa
34070 $_{8;51}$	64	245	-	200	24.29	110.9	29.28	4.00	4.30
34070 $_{11;41}$	72	200	-	200	27.29	110.9	27.29	2.75	3.15
34070 $_{18;55}$	81	275	-	200	30.33	110.9	38.65	4.00	4.50
37070 $_{18;39}$	72	210	-	200	20.04	110.9	21.15	3.70	4.00
38363 $_{1;31}$	60	150	-	80	11.90	110.9	19.66	2.10	2.35
38363 $_{5;41}$	67	210	300	80	9.30	110.9	23.71	3.20	3.65
201278 $_{7;8}$	65	60	152	20	4.63	110.9	9.07	1.40	1.45
201278 $_{8;15}$	58	70	98	20	7.12	110.9	12.66	1.40	1.55
201278 $_{B1;24}$	67	125	505	40	5.19	110.9	14.61	2.50	2.70
203695 $_{23;24}$	57	109	-	55	9.30	110.9	15.28	1.40	1.65
203949 $_{7;25}$	64	115	216	115	13.25	110.9	13.25	1.60	1.80
203949 $_{7;29}$	56	145	209	135	12.79	110.9	13.89	1.76	2.00
204296 $_{1;37}$	60	170	-	150	20.80	110.9	23.02	3.93	4.00
204296 $_{6;21}$	62	110	195	70	9.83	110.9	14.26	2.56	2.70
204296 $_{9;21}$	70	112	160	90	9.28	110.9	11.71	2.45	2.60
204296 $_{22;11}$	56	75	148	65	5.74	110.9	6.85	1.05	1.10
204296 $_{22;27}$	81	150	261	130	11.45	110.9	13.67	2.05	2.25
204607 $_{2;6}$	78	40	48	25	4.19	110.9	5.85	0.75	0.80
204607 $_{5;7}$	100	37	66	25	4.44	110.9	5.77	1.20	1.25
204607 $_{6;9}$	66	57	93	25	4.41	110.9	7.96	1.40	1.47
204608 $_{1;34}$	76	173	361	150	14.11	110.9	16.66	2.60	2.90
204608 $_{7;16}$	57	98	135	70	8.21	110.9	11.32	1.73	1.85
205231 $_{1;12}$	64	70	75	50	7.72	110.9	9.94	1.55	1.65
205231 $_{1;20}$	62	100	131	70	8.50	110.9	11.83	2.33	2.50
206374 $_{1;17}$	45	95	150	70	12.95	110.9	15.72	1.75	1.85
206374 $_{1;25}$	57	130	269	90	10.97	110.9	15.41	1.90	2.20

Geo ID	I_P	σ'_{v0}	σ'_{swell}	$\sigma'_{v,min}$	E_{OED}	a	E_{OED_insitu}	q_{net}	q_c
	%	kPa	kPa	kPa	MPa		MPa	MPa	MPa
202082 $_{B9;51}$	182	247	341	220	13.18	67.4	15.00	2.45	2.90
202082 $_{5;71}$	110	335	445	300	41.79	139.0	46.66	6.72	7.35
202082 $_{17;41}$	125	200	259	180	15.28	124.1	17.76	2.80	3.15
202082 $_{17;61}$	189	290	406	270	16.24	60.4	17.45	3.00	3.52
202082 $_{B9;31}$	66	160	218	140	29.61	182.8	33.27	3.30	3.58
202082 $_{B42}$	85	207	445	180	47.97	163.9	52.39	6.50	6.90
202082 $_{B100}$	142	470	445	430	61.62	107.2	65.91	6.10	7.00
202082 $_{B5;32}$	79	162	445	180	32.77	169.8	29.71	7.20	7.50
202082 $_{B5;62}$	108	298	445	270	56.86	141.0	60.81	4.80	5.35
202082 $_{B5;92}$	101	430	445	400	56.84	148.0	61.28	7.50	8.25
37723 $_{B31}$	77	140	167	150	20.48	171.8	18.76	3.45	3.75
37723 $_{B51}$	250	240	259	200	7.54	-0.2	7.53	2.35	2.90
37723 $_{14;51}$	222	240	-	40	9.89	27.6	15.41	4.91	5.00
37723 $_{17;41}$	112	200	-	40	13.47	137.0	35.40	2.44	2.80
37723 $_{17;61}$	164	280	-	40	7.72	85.3	28.19	3.20	3.70
37509 $_{BH103;3}$	95	158	-	150	23.90				
37509 $_{BH103,21}$	152	251	-	150	25.07				
37509 $_{BH103;27}$	151	312	-	150	34.50				
37509 $_{BH103;33}$	123	384	-	250	64.60				
37509 $_{TR103;64}$	141	145	-	150	21.58				
37509 $_{TR103;80}$	170	221	-	150	21.20				
201278 $_{B2;5}$	121	120	252	40	9.23	128.1	19.47	2.30	2.55
201278 $_{B8;51}$	122	250	505	80	25.76	127.1	47.36	4.00	4.50
201278 $_{B2;30}$	93	150	-	40	14.19	155.9	31.34	4.70	4.95
38363 $_{B41}$	116	190	275	80	15.82	133.0	30.46	3.20	3.60
202826 $_{B43}$	136	210	230	120	10.38	113.2	20.57	2.45	2.70
202826 $_{B53}$	99	250	250	150	20.97	150.0	35.96	6.95	6.65
202826 $_{B31}$	85	150	145	75	11.34	163.9	23.63	1.20	1.47
202728 $_{B7}$	128	130	156	100	11.33	121.1	14.96	1.16	1.33
203949 $_{7;37}$	90	175	400	150	27.86	158.8	31.83	5.20	5.25
203949 $_{7;45}$	87	210	550	180	44.81	161.5	49.66	6.50	6.80
203949 $_{7;53}$	123	240	450	220	27.58	126.2	30.10	4.20	4.45
203949 $_{7;61}$	106	270	320	250	60.73	143.3	63.59	6.70	6.80
204296 $_{B101}$	132	424	503	380	38.45	117.3	43.61	5.80	6.30
204296 $_{6;53}$	112	235	363	150	21.84	137.0	33.49	6.00	6.05
204296 $_{6;77}$	192	333	-	300	28.91	57.5	30.81	4.70	5.20
204296 $_{6;85}$	169	365	457	300	22.70	80.3	27.92	4.70	5.20
204296 $_{9;37}$	79	175	229	150	45.90	169.8	50.14	5.75	5.65
204296 $_{9;53}$	115	240	282	210	30.94	134.0	34.96	4.90	4.85
204296 $_{9;69}$	108	305	340	280	61.60	141.0	65.13	6.00	6.20
204296 $_{9;99}$	119	425	467	380	52.26	130.1	58.11	4.80	5.40
204296 $_{9;85}$	183	370	399	330	34.14	66.4	36.80	5.00	5.50
204296 $_{22;44}$	99	220	285	200	34.65	150.3	37.66	5.10	5.50
204608 $_{B58}$	131	270	333	250	27.64	118.1	30.01	5.40	5.55
204608 $_{B66}$	100	300	404	250	47.77	149.3	55.23	6.50	6.50
204608 $_{B82}$	110	365	461	300	41.68	139.0	50.72	9.70	9.40
204608 $_{B98}$	162	429	550	350	30.97	87.0	37.85	5.00	5.65
205231 $_{B28}$	98	135	150	100	18.50	151.0	23.79	3.20	3.40
205231 $_{B44}$	67	200	250	150	68.35	182.2	77.46	5.75	6.15
206374 $_{B49}$	112	235	279	160	18.48	137.0	28.76	4.00	4.45
206374 $_{B65}$	170	305	53	200	35.61	79.3	43.94	3.40	4.00
206374 $_{B73}$	110	340	452	275	73.53	139.0	82.57	9.30	10.0
206374 $_{B89}$	192	406	650	350	24.80	57.5	28.01	5.20	6.05

Figure 6. Test results for Septarian Clays (left) and Søvind Marl (right).

Consequently, E_{OED} depends on the in situ stress level and must be corrected in case $\sigma'_{v,min}$ deviates from σ'_{v0} when correlated with the tip cone resistance at the same level. Alternatively, the tip cone resistance should refer to the level where the vertical effective in situ stress is equal to the minimum unloading stress from the test. Due to the wildly fluctuating q_{net} cf. Figure 1, the first option should be chosen.

Table 1. Natural water content (w_{nat}) and plasticity index (I_P) of the test samples.

Soil type	Property	Min	Max	Mean
Søvind Marl	w_{nat} (%)	30	52	39
	I_P (%)	66	250	125
Septarian Clays	w_{nat} (%)	24	54	36
	I_P (%)	45	100	64

For the Septarian Clays, the correction is done using Eq. (2) where a is the slope of the trend line in Figure 7.

$$E_{OED\_insitu} \approx E_{OED} + a\ (\sigma'_{v\_insitu} - \sigma'_{v\_min}) \quad (2)$$

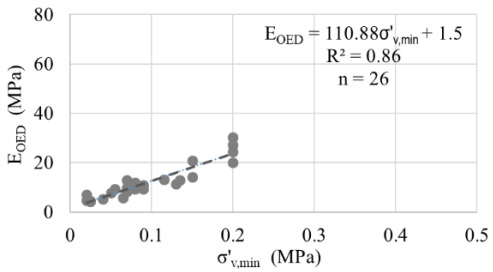

Figure 7. Correlation between minimum vertical effective unloading stress and re-loading stiffness.

According to Figure 7 the slope $a \approx 110.88$. Figure 6 list the associated in situ E_{OED}'s.

The reload stiffness E_{OED} from the Søvind Marl tests is presented in Figure 6 and recorded in Figure 8 as a function of the minimum unloading stress $\sigma'_{v,min}$ during testing. According to figure 8, the correction factor depend highly on plasticity.

The trend line for I_P *(%)* versus a in Figure 8 indicate a correction factor $a \approx 248.42 - 0.9946 \cdot I_P(\%)$ for Søvind Marl. Figure 6 list the associated in situ E_{OED}'s.

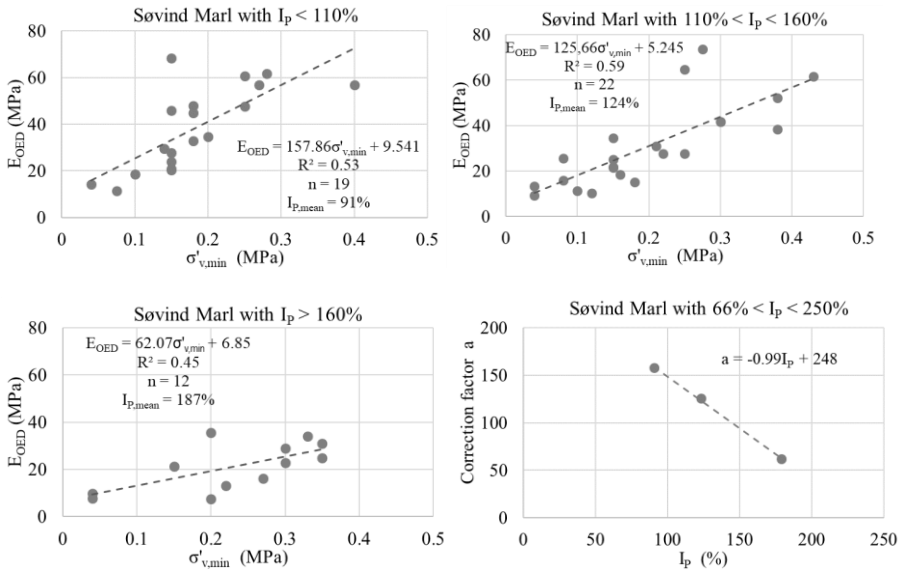

Figure 8. Correlation between minimum vertical effective unloading stress and re-loading stiffness and its dependence on plasticity.

4. CORRELATING CONE RESISTANCE TO E_{OED}

Scatter plots between q_c and E_{OED} as well as between q_{net} and E_{OED} are presented in Figure 9. The cone resistance is measured in a nearby CPTu at the same level from which the sample for the oedometer test was taken.

The CPT's are typically performed two meters from the borehole. However due to the inevitable deflection, the distance may be many times larger at the base of the CPT stroke. The distance introduces uncertainty and thus scatter when the CPT measurements are correlated with measured soil parameters from in situ testing or laboratory testing on soil samples extracted from the boring. Consequently, a relatively large number of tests is required to achieve a satisfactory strong correlation.

With reference to Lunne et al. (1997) a simple linear correlation is chosen. The trend lines indicate Aarhus correlations between the four data sets as presented in equation (3)-(6).

Septarian Clays: $E_{OED} = 6.6\ q_c$ (3)

Søvind Marl: $E_{OED} = 7.3\ q_c$ (4)

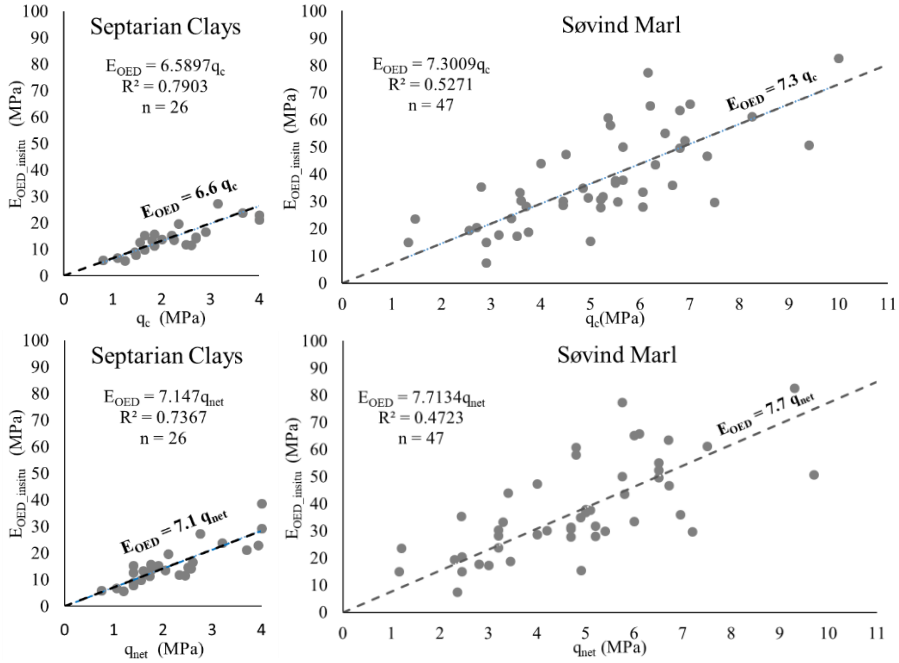

Figure 9. Correlations between q_c and E_{OED} (above) and q_{net} and E_{OED} (below).

A confidence interval for the q_c-proportionality factor is computed to be CI(95) = 6.6±0.6 and 7.3±0.8, respectively.

Septarian Clays: $E_{OED} = 7.1\ q_{net}$ (5)

Søvind Marl: $E_{OED} = 7.7\ q_{net}$ (6)

A confidence interval for the q_{net}-proportionality factor is computed to be CI(95) = 7.1±0.7 and 7.7±0.9, respectively.

As seen from Figure 9, the R^2-values indicate that correlation is somewhat better for the Septarian Clays than for the Søvind Marl. This is probably because the tip resistance and thus soil stiffness, fluctuates significantly much more in Søvind Marl, cf. Figure 1. It also appears that the correlations with q_c are stronger than the correlations with q_{net}.

Figure 10 compares E_{OED} calculated with correlation algorithms (3) - (6) with the derived E_{OED_insitu} values from Figure 6 to evaluate the correlations. As can be seen, the error using the algorithms for the Septarian Clays is symmetric throughout the validity range ($0.8 < q_c$ or q_{net} (MPa) < 4) for both q_c and q_{net}. However for the Søvind Marl, there is a small systematic deviation throughout the validity range ($1.2 < q_c$ or q_{net} (MPa) < 10), but taking into account the greater scatter, the deviation is considered acceptable - especially for q_c.

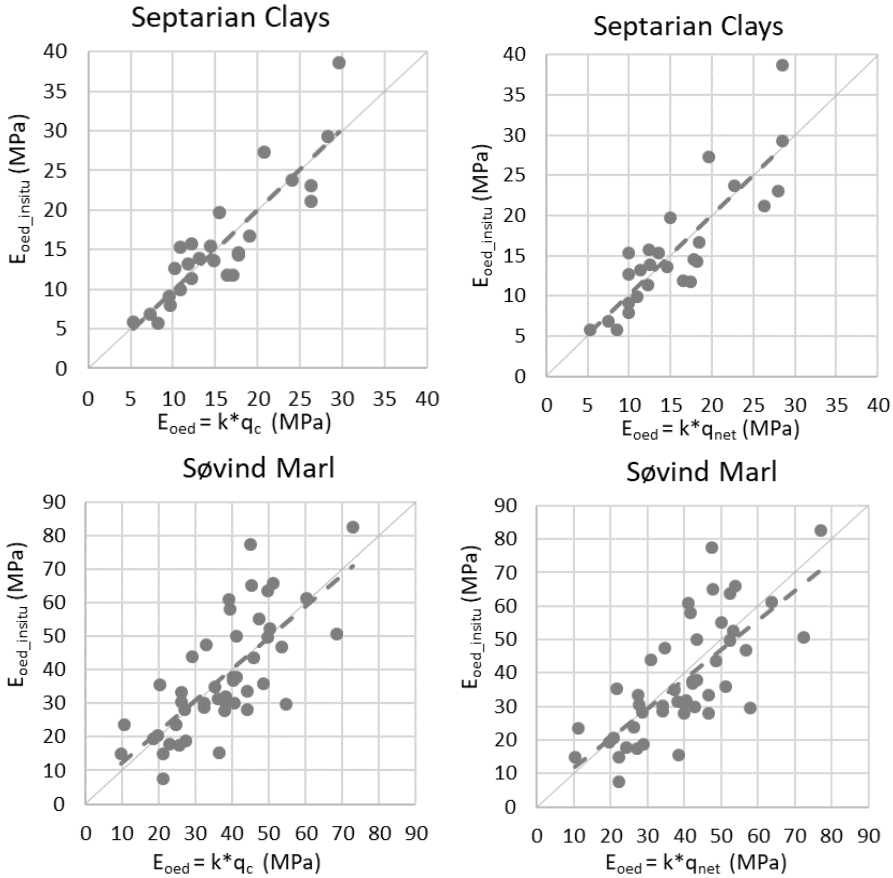

Figure 10. Correlation algorithm check.

5. SUMMARY AND CONCLUSION

Geo has determined the reloading oedometer stiffness E_{OED} from 26 oedometer tests with Septarian Clays and 46 oedometer tests with Søvind Marl in connection with geotechnical surveys for high-rise buildings in Aarhus. This paper demonstrate that simple linear functions of only the cone tip resistance q_c, or the net-corrected resistance q_{net}, can predict the reloading oedometer stiffness in highly over-consolidated, fissured, marine Paleogene clays and marls of very high plasticity. The derived Aarhus correlations are presented in equations (3), (4), (5), and (6).

The prediction accuracy is found very satisfactory for practical use given the unpredictability of the soils. The interval of validity of the correlations is documented in Septarian Clay for tip resistances $0.8 < q_c$ or $q_{net} < 4$ MPa, meanwhile in Søvind Marl for $1.2 < q_c$ or $q_{net} < 10$ MPa.

The performances appear best with q_c, which may most likely be due to the additional associated uncertainties related to the data acquisition of the excess pore water pressure and the overburden pressure needed for the derivation of q_{net}.

The proposed correlations make it possible to transform CPTu-profiles in to E_{OED}-profiles for use in the preliminary analysis of deformations. More importantly, the correlations support the final derivation of E_{OED} for 3D finite element models once the results of all field and laboratory tests for the construction project are available.

The derived correlations complements corresponding Aarhus correlations between q_c or q_{net} and the drained triaxial unloading and reloading stiffness E_{ur} [4] and the maximum small-strain shear modulus G_0 as well [5].

REFERENCES

[1] R. B. J. Brinkgreve and P. A. Vermeer: PLAXIS-Finite element code for soil and rock analysis, Plaxis 3D. Manuals, Delft University of Technology & Plaxis bv, The Netherlands, 2015.

[2] M. H. Jacobsen: New oedometer and new triaxial apparatus for firm soils, The Danish Geotechnical Institute (Geo), bull. No. 27, Copenhagen, 1970.

[3] T. Lunne, P. K. Robertson and J. J. M. Powell: Cone Penetration testing in geotechnical practice. Blackie academic & professional, 1997. https://doi.org/10.1201/9781482295047

[4] N. Okkels, L. Bødker and T. Thorsen: Correlating q_{net} to E_{ur} of Paleogene clays of very high plasticity. Proceedings of the XVIII ECSMGE, Lisbon, 2024.

[5] E. Skouboe, N. Okkels, K. H. Lundvig: Correlating CPTu data to G_0 in highly over-consolidated Paleogene clays of very high plasticity. Proceedings of the XVIII ECSMGE, Lisbon, 2024.

[6] L. Thøgersen: Effects of Experimental Techniques and Osmotic Pressure on the Measured Behaviour of Tertiary Expansive Clay. Ph.D. Thesis. Aalborg University, 2001.